

## ORIGINAL ARTICLE

# *Antrodia cinnamomea* reduces obesity and modulates the gut microbiota in high-fat diet-fed mice

C-J Chang<sup>1,2,3,4,14</sup>, C-C Lu<sup>5,14</sup>, C-S Lin<sup>1,2,3,4,14</sup>, J Martel<sup>1,2</sup>, Y-F Ko<sup>6,7</sup>, DM Ojcius<sup>1,2,8</sup>, T-R Wu<sup>3</sup>, Y-H Tsai<sup>3</sup>, T-S Yeh<sup>9</sup>, J-J Lu<sup>3,10</sup>, H-C Lai<sup>1,2,3,4,10,11,12</sup> and JD Young<sup>1,2,6,7,13</sup>

**BACKGROUND:** Obesity is associated with gut microbiota dysbiosis, disrupted intestinal barrier and chronic inflammation. Given the high and increasing prevalence of obesity worldwide, anti-obesity treatments that are safe, effective and widely available would be beneficial. We examined whether the medicinal mushroom *Antrodia cinnamomea* may reduce obesity in mice fed with a high-fat diet (HFD).

**METHODS:** Male C57BL/6J mice were fed a HFD for 8 weeks to induce obesity and chronic inflammation. The mice were treated with a water extract of *A. cinnamomea* (WEAC), and body weight, fat accumulation, inflammation markers, insulin sensitivity and the gut microbiota were monitored.

**RESULTS:** After 8 weeks, the mean body weight of HFD-fed mice was  $39.8 \pm 1.2$  g compared with  $35.8 \pm 1.3$  g for the HFD+1% WEAC group, corresponding to a reduction of 4 g or 10% of body weight ( $P < 0.0001$ ). WEAC supplementation reduced fat accumulation and serum triglycerides in a statistically significant manner in HFD-fed mice. WEAC also reversed the effects of HFD on inflammation markers (interleukin-1 $\beta$ , interleukin-6, tumor necrosis factor- $\alpha$ ), insulin resistance and adipokine production (leptin and adiponectin). Notably, WEAC increased the expression of intestinal tight junctions (zonula occludens-1 and occludin) and antimicrobial proteins (Reg3g and lysozyme C) in the small intestine, leading to reduced blood endotoxemia. Finally, WEAC modulated the composition of the gut microbiota, reducing the Firmicutes/Bacteroidetes ratio and increasing the level of *Akkermansia muciniphila* and other bacterial species associated with anti-inflammatory properties.

**CONCLUSIONS:** Supplementation with *A. cinnamomea* produces anti-obesogenic, anti-inflammatory and antidiabetic effects in HFD-fed mice by maintaining intestinal integrity and modulating the gut microbiota.

*International Journal of Obesity* (2018) 42, 231–243; doi:10.1038/ijo.2017.149

## INTRODUCTION

Obesity is associated with reduced longevity and poor quality of life.<sup>1</sup> The prevalence of overweight and obesity has increased in developed and developing countries in recent years.<sup>2</sup> Epidemiological evidence suggests that obesity is closely associated with many chronic diseases, including type 2 diabetes mellitus, cancer and cardiovascular disease.<sup>3</sup> For these reasons, the treatment of obesity and its complications has become a major public health issue and novel treatment strategies would be highly beneficial.

The adipose tissues of obese individuals secrete pro-inflammatory cytokines—also called adipokines—which include tumor necrosis factor- $\alpha$  (TNF- $\alpha$ ), interleukin (IL)-1 $\beta$ , IL-6 and monocyte chemoattractant protein-1 (MCP-1).<sup>4</sup> Pro-inflammatory adipokines not only promote systemic inflammation but also insulin resistance which is associated with the development of type 2 diabetes.<sup>3</sup> Regulation of adipokine expression is thus critical

to reduce chronic inflammation and insulin resistance in obese animals and humans.

Medicinal mushrooms have been widely used as folk medicine in Asia for the prevention and treatment of human diseases.<sup>5,6</sup> *Antrodia cinnamomea* Chang and Chou (also called *Antrodia camphorata* or *Taiwanofungus camphoratus*) is a rare and unique fungus that is found in the forests of Taiwan.<sup>7</sup> Previous studies have shown that *A. cinnamomea* possesses anti-cancer,<sup>8</sup> immunomodulatory<sup>9</sup> and hepato-protective properties.<sup>10</sup> We showed earlier that an ethanol extract of *A. cinnamomea* suppresses NLRP3 inflammasome activation and secretion of pro-inflammatory IL-1 $\beta$  and IL-18 in macrophages.<sup>11</sup> *A. cinnamomea* also reduces plasma triglycerides, low-density lipoproteins and total cholesterol in obese hamsters.<sup>12</sup> Similarly, ergostatrien-3 $\beta$ -ol, a compound isolated from an ethanol extract of *A. cinnamomea*, reduces body weight, hyperlipidemia and diabetes symptoms in mice fed with a high-fat diet (HFD).<sup>13</sup> In addition, the triterpenoid

<sup>1</sup>Center for Molecular and Clinical Immunology, Chang Gung University, Taoyuan, Taiwan; <sup>2</sup>Chang Gung Immunology Consortium, Linkou Chang Gung Memorial Hospital, Taoyuan, Taiwan; <sup>3</sup>Department of Medical Biotechnology and Laboratory Science, College of Medicine, Chang Gung University, Taoyuan, Taiwan; <sup>4</sup>Research Center of Bacterial Pathogenesis, Chang Gung University, Taoyuan, Taiwan; <sup>5</sup>Department of Respiratory Therapy, Fu Jen Catholic University, New Taipei City, Taiwan; <sup>6</sup>Chang Gung Biotechnology Corporation, Taipei, Taiwan; <sup>7</sup>Biochemical Engineering Research Center, Ming Chi University of Technology, New Taipei City, Taiwan; <sup>8</sup>Department of Biomedical Sciences, University of the Pacific, Arthur Dugoni School of Dentistry, San Francisco, CA, USA; <sup>9</sup>Department of Surgery, Linkou Chang Gung Memorial Hospital, Taoyuan, Taiwan; <sup>10</sup>Department of Laboratory Medicine, Linkou Chang Gung Memorial Hospital, Taoyuan, Taiwan; <sup>11</sup>Research Center for Chinese Herbal Medicine, College of Human Ecology, Chang Gung University of Science and Technology, Taoyuan, Taiwan; <sup>12</sup>Research Center for Food and Cosmetic Safety, College of Human Ecology, Chang Gung University of Science and Technology, Taoyuan, Taiwan and <sup>13</sup>Laboratory of Cellular Physiology and Immunology, Rockefeller University, New York, NY, USA. Correspondence: Dr H-C Lai, Department of Medical Biotechnology and Laboratory Science, College of Medicine, Chang Gung University, 259 Wen-Hwa First Road, Gueishan 33302, Taoyuan, Taiwan or Dr JD Young, Center for Molecular and Clinical Immunology, Chang Gung University, 259 Wen-Hwa First Road, Gueishan 33302, Taoyuan, Taiwan. E-mail: hclai@mail.cgu.edu.tw or jdyoung@mail.cgu.edu.tw

<sup>14</sup>These authors contributed equally to this work.

Received 13 March 2017; revised 7 May 2017; accepted 7 June 2017; accepted article preview online 20 June 2017; advance online publication, 8 August 2017

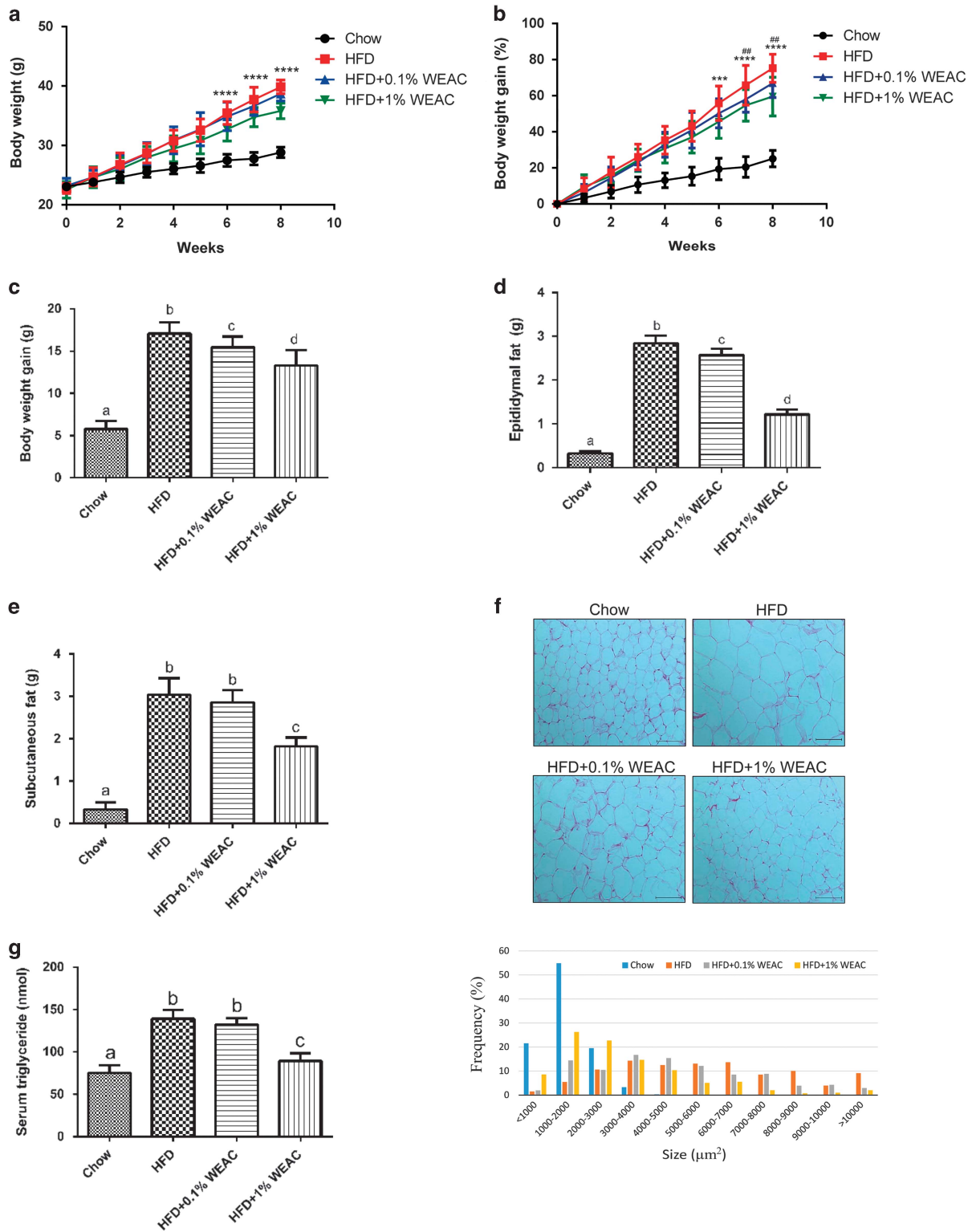


**Figure 1.** WEAC supplementation reduces body weight and fat accumulation in HFD-fed mice. Chow-fed mice ( $n=21$ ) and HFD-fed mice ( $n=15$ ) were treated daily with 200  $\mu$ l of either double-distilled water as control or WEAC at 0.1% ( $n=15$ ) or 1% (w/v) ( $n=15$ ) by intragastric gavage for 8 weeks. Effects of WEAC treatment on body weight (**a**), relative and absolute body weight gain (**b** and **c**), epididymal fat (**d**), subcutaneous fat (**e**), epididymal adipocyte size (**f**) and serum triglycerides (**g**). Parameters shown in **c–g** were measured after eight weeks of feeding. In **f**, adipocyte size was estimated using Adiposoft from the ImageJ software. Scale bars, 50  $\mu$ m. Data are expressed as means  $\pm$  s.d. from three independent experiments. Body weight differences in **a** and **b** were analyzed using two-way ANOVA Bonferroni *post hoc* test ( $^{##}P < 0.01$  for HFD+0.1% WEAC vs HFD;  $^{***}P < 0.001$  and  $^{****}P < 0.0001$  for HFD+1% WEAC vs HFD). Graph bars with different letters on top correspond to statistically significant results ( $P < 0.05$ ) based on Bonferroni *post hoc* one-way ANOVA analysis.

compound dehydroeburicoic acid isolated from *A. cinnamomea* shows antidiabetic and anti-hyperlipidemia activities in streptozotocin-induced diabetic mice.<sup>14</sup> Although these observations suggest that *A. cinnamomea* may contain hydrophobic compounds that produce anti-obesity effects, the effects and mechanism of action of *A. cinnamomea* water extract on HFD-fed mice have not been examined in detail so far.

Recent studies indicate that the gut microbiota is involved in the development of obesity in animals and humans.<sup>15</sup> The community of intestinal microbiota is involved in energy regulation, vitamin production and nutrient harvest.<sup>16</sup> In obese mice, the intestinal microbiota community contains a larger population of Firmicutes and a smaller proportion of Bacteroidetes compared with lean animals.<sup>15</sup> A recent study has shown that the gut microbiota of human obese twins induces weight gain and fat deposition following transplantation into mice fed with a low-fat diet.<sup>17</sup> Moreover, the bacterium *Akkermansia muciniphila* protects against obesity and inflammation in HFD-fed mice by improving intestinal barrier integrity and altering adipose tissue metabolism.<sup>18</sup> In addition to changes produced in the gut microbiota, HFD feeding for 4 weeks reduces intestinal integrity and increases endotoxemia owing to the translocation of bacterial lipopolysaccharides (LPS) from the gut microbiota into the blood.<sup>19</sup> LPS found in the blood in turn induces systemic low-grade inflammation and insulin resistance.<sup>20</sup>

Targeting the gut microbiota with antibiotics, prebiotics and probiotics has been shown to produce beneficial effects on obesity.<sup>21</sup> For instance, specific antibiotic treatment modulates the gut microbiota and reduces obesity, endotoxemia and the cecal content of LPS in both HFD-fed mice and leptin-deficient mice.<sup>19</sup> Administration of probiotics affects host energy metabolism and signaling, and reduces white adipose tissues and blood endotoxemia in HFD-fed mice.<sup>22</sup> Prebiotics are non-digestible, fermentable carbohydrates and fibers that reduce body weight and exert anti-inflammatory effects, mainly by enhancing the growth of beneficial bacteria found in the gut.<sup>23</sup> Prebiotics treatment not only alters the structure of the gut microbiota but also improves intestinal permeability and systemic endotoxemia.<sup>24</sup> In a previous study, we showed that polysaccharides isolated from the medicinal mushroom *Ganoderma lucidum* act as prebiotics and reduce obesity and inflammation by modulating the composition of the gut microbiota.<sup>25</sup> Our previous study prompted us to examine the effects of herbal remedies and medicinal mushrooms on obesity and type 2 diabetes.<sup>26</sup>

In the present study, we show that a water extract of *A. cinnamomea* (WEAC) reduces body weight, insulin resistance and inflammation in HFD-fed mice. WEAC treatment not only maintains intestinal barrier integrity but also modulates the gut microbiota, increasing *A. muciniphila* and other bacterial species associated with anti-inflammatory effects. Our findings thus demonstrate that WEAC may be useful for the treatment of obesity and its complications.

## MATERIALS AND METHODS

### Preparation of *A. cinnamomea* water extract

The *A. cinnamomea* strain used in the present study was initially selected and characterized by Chang Gung Biotechnology. Based on PCR analysis and sequencing of rDNA and internal transcribed spacers (ITS-1 and ITS-2), the strain showed 99.7% homology with a type strain (BCRC strain AJ496398; Bioresource Collection and Research Center, Hsinchu, Taiwan). WEAC was prepared by adding 400 g of dried *A. cinnamomea* mycelium powder (containing 1.5% polysaccharides and 5% triterpenoids) into 10 liters of double-distilled water, followed by incubation at 122 °C for 30 min with gentle agitation. The mixture was centrifuged at 5900 g for 30 min at 4 °C and the supernatant was concentrated using a vacuum centrifuge to obtain a final volume of 2 liters. The solution was autoclaved at 121 °C for 20 min. To determine the final concentration of water-soluble material found in the WEAC solution, the solvent was evaporated and the weight of

the residual material was determined (10%, w/v or 10 g per 100 ml). For the experiments, WEAC was diluted at 0.1% and 1% (w/v) as indicated in the figures.

### Animals

Eight-week-old male C57BL/6J mice with similar initial body weight were randomly assigned to four groups (15–21 animals per group) maintained in groups of three to five animals per cage. (See the figure legends for the number of animals or samples used in each experiment). We placed mice on standard chow diet (13.5% of energy from fat; LabDiet 5001; LabDiet, St Louis, MO, USA) and high-fat diet (60% of energy from fat; TestDiet 58Y1; TestDiet, St Louis, MO, USA) for 8 weeks and monitored body weight. Mice were fed with either chow diet or HFD combined with daily administration of 200 µl of either water or WEAC at 0.1% or 1% (w/v) by intragastric gavage, corresponding to doses of 0.009 and 0.09 g kg<sup>-1</sup> per day, respectively (the average mouse body weight at the start of the experiment was 22.6 g; see Figures 1a, Week 0). The organs, tissues and serum samples of each mouse were collected for subsequent analyses done without blinding. No animals were excluded from the analyses. Animals were housed and treated according to a protocol approved by the Institutional Animal Care and Use Committee of Chang Gung University (IACUC; Approval No. CGU15-006). All experiments were performed according to the guidelines.

### Antibodies

Primary antibodies against Akt (clone C67E7; #4691), phosphorylated Akt (P-Akt; phosphorylation on serine 473; clone D9E; #4060), nuclear factor of kappa light polypeptide gene enhancer in B cells inhibitor alpha (IκB-α; #9242), JNK (c-Jun N-terminal; #9252), phosphorylated JNK (phosphorylation on threonine 183 and tyrosine 185; clone 81E11, #4668), total 5' adenosine monophosphate-activated protein kinase-α (T-AMPK-α; clone 23A3, #2603) and phosphorylated AMPK-α (P-AMPK-α; phosphorylation on threonine 172; clone 40H9; #2535) were purchased from Cell Signaling (Danvers, MA, USA) and diluted 1:1000. Antibodies against β-actin (NB600-501) and horseradish peroxidase-conjugated secondary anti-mouse immunoglobulin G (sc-2005) were purchased from Novus Biologicals (Littleton, CO, USA) and Santa Cruz Biotechnology (Santa Cruz, CA, USA), respectively and diluted 1:20000. Fluorescein-isothiocyanate-conjugated anti-F4/80 antibody (clone BM8; #11-4801; eBioscience, San Diego, CA, USA) and phycoerythrin-conjugated anti-CD11c antibody (clone HL3; #557401; 1:100; BD Pharmingen, San Diego, CA, USA) were also used.

### Biochemical analyses

Serum LPS was quantified using a commercial kit based on the guidelines provided by the supplier (Lal limulus amoebocyte lysate assay; Cambrex Bio Science, East Rutherford, NJ, USA). Serum free fatty acids (Biovision, Milpitas, CA, USA), adiponectin (Biovision) and leptin (mouse leptin ELISA; Abcam, Cambridge, MA, USA) were determined using commercial detection kits. Serum triglycerides were quantified using a commercial detection kit (Biovision). Serum IL-1β, IL-6 and TNF-α were examined with commercial ELISA kits according to manufacturer's instructions (R&D Systems, Minneapolis, MN, USA).

### Analysis of adipose tissues

Epididymal adipose tissues were fixed in 10% formalin overnight. Fixed tissues were treated with paraformaldehyde and processed to obtain paraffin-embedded tissues. Haematoxylin and eosin solution were used to stain sections (5 µm), followed by observation under optical microscopy. Adipocyte size was estimated using Adiposoft from the ImageJ software (National Institutes of Health, USA).

### Determination of energy and fat content in feces

Fecal lipids were extracted as before.<sup>27</sup> In brief, a mixture of heptane/diethylether/ethanol (1:1:1) was vortexed with dried feces once, followed by two homogenization steps with a solution of heptane/diethylether/ethanol/water (1:1:1:1). Collected supernatants were put into weighted vials. The solvent was evaporated and the amount of lipids in each supernatant was determined gravimetrically. Lipid amounts were expressed as percentage of the weight of the starting sample. Energy in feces (kJ g<sup>-1</sup> feces) was measured as reported previously using a bomb calorimeter (Gallenkamp, Loughborough, UK).<sup>25</sup>

### Oral glucose and insulin tolerance tests

The mice used for the oral glucose tolerance test were fasted overnight. Mice were given glucose by oral gavage ( $1 \text{ g kg}^{-1}$ ). Blood glucose was quantified using a glucose meter (Johnson & Johnson, New Brunswick, NJ, USA) from tail vein blood. To assess insulin tolerance, mice were fasted for 6 hours, prior to intraperitoneal injection of human insulin ( $0.3 \text{ units kg}^{-1}$ ; Actrapid, Novo Nordisk, Bagsvaerd, Denmark). Serum blood glucose was measured prior to insulin injection and every 30 min thereafter. Serum insulin was quantified using a commercial ELISA kit (Mercodia, Uppsala, Sweden).

### Quantitative real-time reverse transcription polymerase chain reaction

RNA level expression analysis was performed using total RNA isolated using a commercial kit (Geneaid, New Taipei City, Taiwan). RNA was used for reverse transcription with Quant II fast reverse transcriptase kit (Tools, Taipei, Taiwan). The resulting cDNA ( $1.5 \mu\text{l}$ ) was used as template and mixed with  $1 \mu\text{l}$  of target primers,  $5 \mu\text{l}$  of KapaSYBR Fast Master Mix and  $2.5 \mu\text{l}$  of water in each wells. PCR conditions were as follows: initial pre-incubation at  $95^\circ\text{C}$  for 10 min, 50 PCR cycles of  $94^\circ\text{C}$  for 15 sec,  $60^\circ\text{C}$  for 30 s,  $72^\circ\text{C}$  for 30 s and then one melting curve cycle. The primers used are listed in Supplementary Table 1. Data were analyzed with the Roche LightCycler software (version 1.5.0, Roche Diagnostics, Indianapolis, IN, USA). Relative quantification was performed using the comparative  $2^{-\Delta\Delta C_T}$  method. Expression was normalized against glyceraldehyde 3-phosphate dehydrogenase. Mean expression level of chow-fed mice was set at a value of 1.

### Western blotting

Adipose tissues (100 mg) were collected and homogenized in Pro-Prep Protein Extraction Solution (Intron Biotechnology, Seoul, South Korea). Equal amounts of proteins were separated on a 10% sodium dodecyl sulfate-polyacrylamide gel and transferred onto polyvinylidenedifluoride membranes (Immobilon TM-P; Millipore, Billerica, MA, USA). Membranes were soaked with 5% non-fat milk for 1 h at room temperature in TBST buffer (Tris 10 mM, NaCl 150 mM, pH 7.6, 0.1% Tween 20). Membranes were incubated in 5% BSA containing primary antibodies at  $4^\circ\text{C}$  overnight, followed by incubation with horseradish peroxidase-conjugated secondary antibody. Protein signals were detected using enhanced chemiluminescence (Millipore).

### Flow cytometry analysis

Adipose tissues were minced into fine pieces and digested with collagenase (Sigma, St Louis, MO, USA) in Krebs-Henseleit-HEPES buffer (Sigma; pH 7.4) containing BSA ( $20 \text{ mg ml}^{-1}$ ) and glucose (2 mM). Samples were passed through a  $40 \mu\text{m}$  strainer mesh and centrifuged (1000 g) to obtain stromal-vascular fractions. Cells were pretreated for 30 min with Fc receptors (clone 2.4G2; Becton Dickinson, Franklin Lakes, NJ, USA). Cells were stained for 30 min with primary antibodies or the matching control isotypes at  $4^\circ\text{C}$ . After two washing steps, the labeled cells were analyzed by flow cytometry (FACSCalibur, Becton Dickinson) and the Kaluza software (Beckman Coulter, Brea, CA, USA) was used to analyze flow cytometry data. Macrophages were identified as F4/80 and CD11c double-positive cells.

### Gut microbiota analysis

Cecum feces were snap-frozen in liquid nitrogen and stored at  $-80^\circ\text{C}$ . Cellular DNA was extracted using a fecal DNA isolation kit according to manufacturer's instructions (Qiagen, Redwood City, CA, USA). 16S rRNA gene containing the V3–V4 regions was amplified using composite primers containing a unique 10-base barcode to tag PCR products. The PCR mix ( $50 \mu\text{l}$ ) was prepared as per the instructions of the KAPA HiFi PCR kit (KAPA Biosystems, Wilmington, MA, USA). PCR conditions comprised pre-denaturation at  $95^\circ\text{C}$  for 3 min, followed by 15–25 cycles of  $98^\circ\text{C}$  for 20 s,  $45^\circ\text{C}$  for 15 s and  $72^\circ\text{C}$  for 15 s, and a final extension of  $72^\circ\text{C}$  for 1 min. Composite primers consisted of the forward primer 5'-TCGTCGGCAGCGTCAGATGTGTATAAGAGACAGCCTACGGGNGGCWGCAG-3', which contains the Illumina forward overhang adaptor sequence (underlined) and the universal bacterial primer 341F (italicized), and the reverse primer 5'-GTCTCGTGGGCTCGGAGATGTGTATAAGAGACAGGACTACHVGGGTATCTAATCC-3', which contains the Illumina reverse overhang adaptor sequence (underlined) and the broad-range bacterial primer 805R (italicized). V3–V4 amplicons were purified from the pooled replicate PCRs

using the QiaQuick PCR Purification Kit (Qiagen), followed by sequencing using the Illumina MiSeq pyrosequencer platform as per the instructions of the manufacturer. The paired-end library was constructed with the Ovation Ultralow DR Multiplex System 1–96 (NuGen, San Carlos, CA, USA) based on the manufacturer's instructions. Library concentration and quality were assessed using Bioanalyzer 2100 (Agilent, Palo Alto, CA, USA) and a DNA 1000 lab chip (Agilent). 16S amplicon libraries were sequenced with the  $2 \times 301+8 \text{ bp}$  (index) using MiSeq Reagent kit v3 (600 cycles) on the Illumina MiSeq system following the manufacturer's instructions. Microbiota sequencing data were deposited into NCBI's Sequence Read Archive (accession# SPR106223).

Effective reads from all samples were selected from high-quality reads and clustered into operational taxonomic units (OTUs) based on 97% sequence similarity according to MiSeq standard operating procedures.<sup>28</sup> In brief, high-quality reads were selected by removing sequences that lacked V3–V4 primers or barcode sequences as well as sequences that contained undetermined bases ( $>2$  bases) or a short variable region ( $<90 \text{ bp}$ ) in the V3–V4 region. For reducing noise signals, a 50-bp sliding window was used to reduce sequencing error in combination with an average quality score of 35 within that window for sequence trimming. High-quality sequences were aligned using the nearest alignment space termination multi-aligner in SILVA-compatible database alignment,<sup>29</sup> and reads that were not aligned to the anticipated reference region were deleted, followed by removal of chimera sequences identified using the UCHIME algorithm.<sup>30</sup> All reads were classified using a Bayesian classifier with a homemade RDP database. Reads that could not be classified at the kingdom level were deleted. Alpha diversity analysis including rarefaction analysis and Shannon index were calculated using QIIME as described before.<sup>31</sup> UniFrac-based principal coordinate analysis was performed and the phylogenetic tree was constructed by inserting the representative of each OTU generated using QIIME.<sup>31</sup> Based on published statistical methods,<sup>22,25</sup> the statistical significance of the separation among animal groups in the principal coordinate analysis score plots was assessed using multivariate analysis of variance test according to UniFrac matrix differences. OTUs with statistically significant differences were analyzed using Tukey's *post hoc* test (SPSS, Chicago, IL, USA).  $\text{Log}_{10}$ -transformed relative abundance of each OTU was used to construct RDA models with Canoco-assessed OTUs that were different between animal groups (Microcomputer Power, Ithaca, NY, USA). Statistical significance was determined using the Monte Carlo Permutation Procedure with 499 random permutations.

### Statistical analysis

Data obtained from three independent experiments are shown as means  $\pm$  s.d. Differences in absolute body weight and body weight gain were determined using two-way analysis of variance Bonferroni *post hoc* test. Data sets involving more than two groups were analyzed using Bonferroni one-way analysis of variance followed by *post hoc* test. Next-generation sequencing analysis was assessed using Tukey's honest significant difference *post hoc* test. *P*-values below 5% were considered statistically significant. The two-stage procedure of Benjamini et al.<sup>32</sup> was used to control the false discovery rate.

## RESULTS

### WEAC reduces HFD-induced obesity in mice

To study the effects of *A. cinnamomea* on obesity, we used an animal model of diet-induced obesity in which mice were fed with a HFD for 8 weeks.<sup>25</sup> HFD feeding for this period led to significant increases in body weight, epididymal and subcutaneous fat accumulation, adipocyte size and serum triglyceride levels compared with the control chow-fed group (Figures 1a–g). Notably, WEAC supplementation significantly decreased body weight and fat accumulation in HFD-fed mice (Figures 1a–g). After 8 weeks of feeding, the mean body weight of the HFD group was  $39.8 \pm 1.2 \text{ g}$  compared with  $35.8 \pm 1.3 \text{ g}$  for the HFD+1% WEAC group (Figure 1a), corresponding to a difference of 4 g or 10% of body weight ( $P < 0.0001$ ). Although the 0.1% WEAC treatment reduced body weight gain in a statistically significant manner after 7 weeks of feeding (Figure 1b), 1% WEAC reduced body weight and body weight gain after 6 weeks of feeding (Figures 1a and b). WEAC treatments reduced both epididymal and subcutaneous fat after 8 weeks of feeding (Figures 1d and e), although the effects of

0.1% WEAC on subcutaneous fat did not reach statistical significance (Figure 1e). WEAC treatments reduced adipocyte size within epididymal adipose tissues (EAT) (Figure 1f, adipocyte size distribution is shown in the bottom panel). The 1% WEAC treatment also reduced serum triglyceride level compared with control HFD (Figure 1g). Of note, feces energy, food intake and stool fat contents showed no statistically significant differences between HFD groups (Supplementary Figure 1), indicating that the effects of WEAC on body weight and lipid accumulation were not due to reduction in appetite, lipid absorption, or energy extraction. These results indicate that WEAC supplementation reduces body weight gain and fat accumulation in obese mice.

#### WEAC reduces pro-inflammatory cytokines in HFD-fed mice

Previous studies have shown that the adipose tissues of obese animals secrete higher levels of pro-inflammatory cytokines compared with the adipose tissues of lean animals.<sup>20</sup> To determine whether WEAC reduces inflammation, we monitored mRNA expression levels of pro-inflammatory cytokines in EAT after 8 weeks of HFD feeding and WEAC supplementation. TNF- $\alpha$ , IL-1 $\beta$  and IL-6 expression levels were higher in HFD-fed mice compared with chow-fed mice (Figures 2a–c). WEAC supplementation (1%) significantly reduced cytokine expression levels compared with the HFD group (Figures 2a–c). Similar to the results obtained for mRNA expression, WEAC supplementation reduced TNF- $\alpha$ , IL-1 $\beta$  and IL-6 protein levels in the blood of HFD-fed mice (Figures 2d–f). These results indicate that WEAC supplementation reduces inflammation markers in obese mice.

#### WEAC reduces inflammation in adipose tissues of HFD-fed mice

One important characteristic of obesity is the infiltration and activation of immune cells in adipose tissues.<sup>33</sup> MCP-1 is a pro-inflammatory cytokine that recruits and activates macrophages in adipose tissues of obese animals.<sup>34</sup> Accordingly, mRNA expression levels of MCP-1 and the macrophage biomarker F4/80 were significantly elevated in EAT of HFD-fed mice compared with chow-fed mice (Figures 3a and b). WEAC supplementation (1%) reduced F4/80 and MCP-1 gene expression levels in HFD-fed mice (Figures 3a and b). We further examined the amount of double-positive F4/80-CD11c macrophages recruited in EAT using flow cytometry analysis. Our results showed that WEAC reduced the infiltration of activated macrophages in a dose-dependent manner in EAT of HFD-fed mice (Figure 3c).

Next, we examined the effects of WEAC supplementation on LPS blood levels. Although the HFD induced a large increase of serum endotoxin, WEAC supplementation (1%) reduced endotoxin level in a statistically significant manner (Figure 3d). LPS has previously been shown to activate JNK and NF- $\kappa$ B signaling pathway and increase expression of pro-inflammatory cytokines in activated macrophages and adipose tissues.<sup>35</sup> We examined whether this pathway was affected by WEAC supplementation in EAT. Phosphorylation (and activation) of JNK was reduced by WEAC (1%) compared with HFD-fed mice (Figure 3e), whereas the amount of I $\kappa$ B- $\alpha$  (an inhibitor of the transcription factor NF- $\kappa$ B) increased in WEAC-treated mice (Figure 3f). Based on these results, we conclude that WEAC supplementation reduces inflammation by decreasing infiltration of activated macrophages and LPS-induced NF- $\kappa$ B and JNK signaling in adipose tissues.

#### WEAC reduces insulin resistance in HFD-fed mice

Previous studies have shown that endotoxemia and chronic inflammation can lead to insulin resistance and type 2 diabetes in mice.<sup>19,20</sup> As expected, WEAC supplementation (1%) reduced fasting insulin and glucose levels in HFD-fed mice (Figures 4a and b). Moreover, WEAC reduced glucose intolerance and increased insulin sensitivity in HFD-fed mice submitted to oral glucose

tolerance test (Figure 4c) and insulin tolerance test, respectively (Figure 4d; graphs showing the area under the curves, or AUC, are also shown in the panels on the right). Previous work<sup>35</sup> has shown that endotoxin-induced activation of JNK and NF- $\kappa$ B signaling pathway may decrease phosphorylation of Akt downstream of the insulin receptor, leading to insulin resistance. Consistent with the insulin-sensitizing effects shown above, WEAC supplementation induced the accumulation of phosphorylated Akt in a dose-dependent manner in EAT of HFD-fed mice (Figure 4e). WEAC therefore reduces insulin resistance in obese mice.

#### WEAC modulates the expression of leptin and adiponectin in HFD-fed mice

Leptin and adiponectin are adipokines that have an important role in modulation of obesity, insulin resistance and related inflammatory disorders.<sup>36</sup> We examined whether the expression and production of leptin and adiponectin in EAT is affected by WEAC supplementation. We observed that leptin expression was elevated in HFD-fed mice compared with chow-fed mice, whereas WEAC reduced leptin expression in HFD-fed mice (Supplementary Figure 2a). In contrast to leptin, adiponectin expression level was lower in HFD-fed mice compared with the chow group, and WEAC supplementation increased adiponectin expression (Supplementary Figure 2b). Of note, WEAC (1%) reversed the effects of the HFD on leptin and adiponectin serum protein levels (Supplementary Figure 2c and d).

The AMPK enzyme, which acts downstream of the adiponectin receptor, reduces inflammation and insulin resistance in HFD-fed mice.<sup>36</sup> As WEAC induced the expression and production of adiponectin in EAT and the serum of HFD-fed mice (Supplementary Figure 2b and d), we examined the phosphorylation status of AMPK in EAT. Phosphorylated (active) AMPK level was reduced in HFD-fed mice, whereas WEAC treatment increased the level of this protein (Supplementary Figure 2e). These results suggest that WEAC supplementation may reduce inflammation and insulin resistance by modulating the activities of leptin and adiponectin.

#### WEAC regulates expression of genes involved in fatty-acid metabolism

Previous studies have shown that the expression of genes involved in fatty-acid biosynthesis, such as acetyl-CoA carboxylase-1 (ACC-1), fatty-acid synthase (FAS) and sterol regulatory element-binding protein-1c (SREBP-1c), are upregulated in adipose tissues of HFD-fed mice, whereas fatty-acid catabolism genes, such as PPAR- $\gamma$  co-activator 1 $\alpha$  (PGC-1 $\alpha$ ), are downregulated.<sup>37</sup> AMPK was also reported to control lipid metabolism by regulating the expression of these four genes.<sup>38</sup> Notably, WEAC supplementation (1%) reduced expression of ACC-1, FAS and SREBP-1c in EAT of HFD-fed mice, whereas it increased the expression of PGC-1 $\alpha$  (Supplementary Figure 3a–d). Previous work showed that free fatty acid levels increase in the blood of obese animals and may enhance inflammation by activating Toll-like receptor-4 on adipocytes and macrophages.<sup>39</sup> Notably, WEAC supplementation (1%) reduced serum free fatty acid levels in HFD-fed mice (Supplementary Figure 3e). Based on these results, WEAC may reduce lipid accumulation by regulating the expression of genes involved in lipid metabolism in HFD-fed mice.

#### WEAC enhances antimicrobial peptide production and maintains intestinal barrier integrity

Antimicrobial peptides produced by intestinal cells have an important role in maintaining gut microbiota homeostasis and physical segregation of commensal microorganisms from host tissues.<sup>40</sup> Previous studies have shown that the expression of antimicrobial peptides, such as Reg3g, lysozyme C and PLA2g2 (phospholipase A2 group II), is reduced in HFD-fed mice.<sup>24</sup>

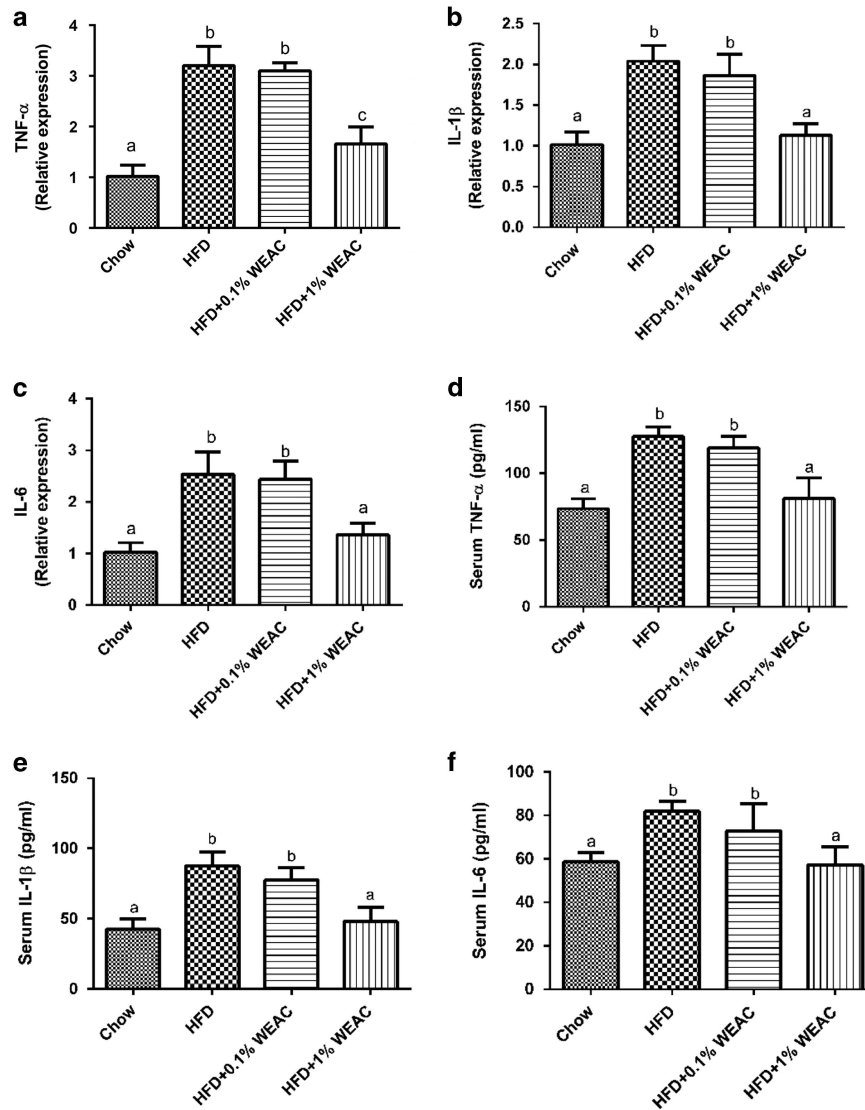


**Figure 2.** WEAC reduces pro-inflammatory cytokine expression and production in HFD-fed mice. Mice were treated as in Figure 1. Relative expression of TNF- $\alpha$  (a), IL-1 $\beta$  (b), and IL-6 (c) in EAT was assessed using qRT-PCR. Expression was normalized against GAPDH. TNF- $\alpha$  (d), IL-1 $\beta$  (e) and IL-6 (f) protein levels in the serum of chow-fed and HFD-fed mice were determined using ELISA ( $n = 5$  for each group). Data are shown as means  $\pm$  s.d. Graph bars with different letters on top correspond to statistically significant results ( $P < 0.05$ ) based on Bonferroni *post hoc* one-way ANOVA analysis.

Notably, we observed that WEAC (1%) increased the expression of Reg3g and lysozyme C in the ileum of HFD-fed mice, whereas PLA2g2 was unaffected (Supplementary Figure 4a–c). We also examined whether WEAC modulates intestinal tight junction proteins, which maintain intestinal barrier integrity. Although HFD feeding reduced expression of zonula occludens-1 and occludin in the ileum, WEAC supplementation increased the expression level of these proteins (Supplementary Figure 4d and e). Consistent with the reduced blood endotoxin level noted above in WEAC-treated mice (Figure 3d), these findings suggest that WEAC attenuates the effects of HFD on host antimicrobial defense and intestinal barrier integrity.

**WEAC alters the diversity and composition of the gut microbiota in HFD-fed mice**

Previous studies have shown that the gut microbiota is involved in the development of lean and obese phenotypes in animals.<sup>17</sup> Reduced bacterial richness and diversity have been observed in obese humans and mice.<sup>25,41</sup> We examined whether WEAC may

alter the composition and diversity of the gut microbiota by analyzing bacterial 16S rRNA (V3–V4 DNA region) in cecal feces using next-generation sequencing. After removing unqualified sequences (see Methods), a total of 5 063 884 raw reads and an average of  $133\,260 \pm 31\,937$  reads per sample were obtained. A total of 2 379 449 effective reads was generated, with each fecal sample ( $n = 4$  for chow, HFD and HFD+0.1%;  $n = 3$  for HFD+1%) producing an average of  $62\,617 \pm 15\,009$  effective reads. Samples with a low number of effective reads ( $< 3000$ ) were discarded. Rarefaction analysis indicated that the sequencing depth covered rare and new phylotypes and broad bacterial diversity.

As shown in Figures 5a–c, the observed species and the two indexes reflecting species richness and diversity (Chao-1 index and Shannon index, respectively) were reduced in HFD-fed mice compared with chow-fed mice, consistent with previous studies.<sup>25</sup> In contrast, the richness and diversity of the gut microbiota of HFD-fed mice were enhanced in a statistically significant manner by 1% WEAC supplementation (Figures 5a–c). UniFrac-based principal coordinates analysis revealed distinct clustering of microbiota composition for each treatment (Figure 6a). In

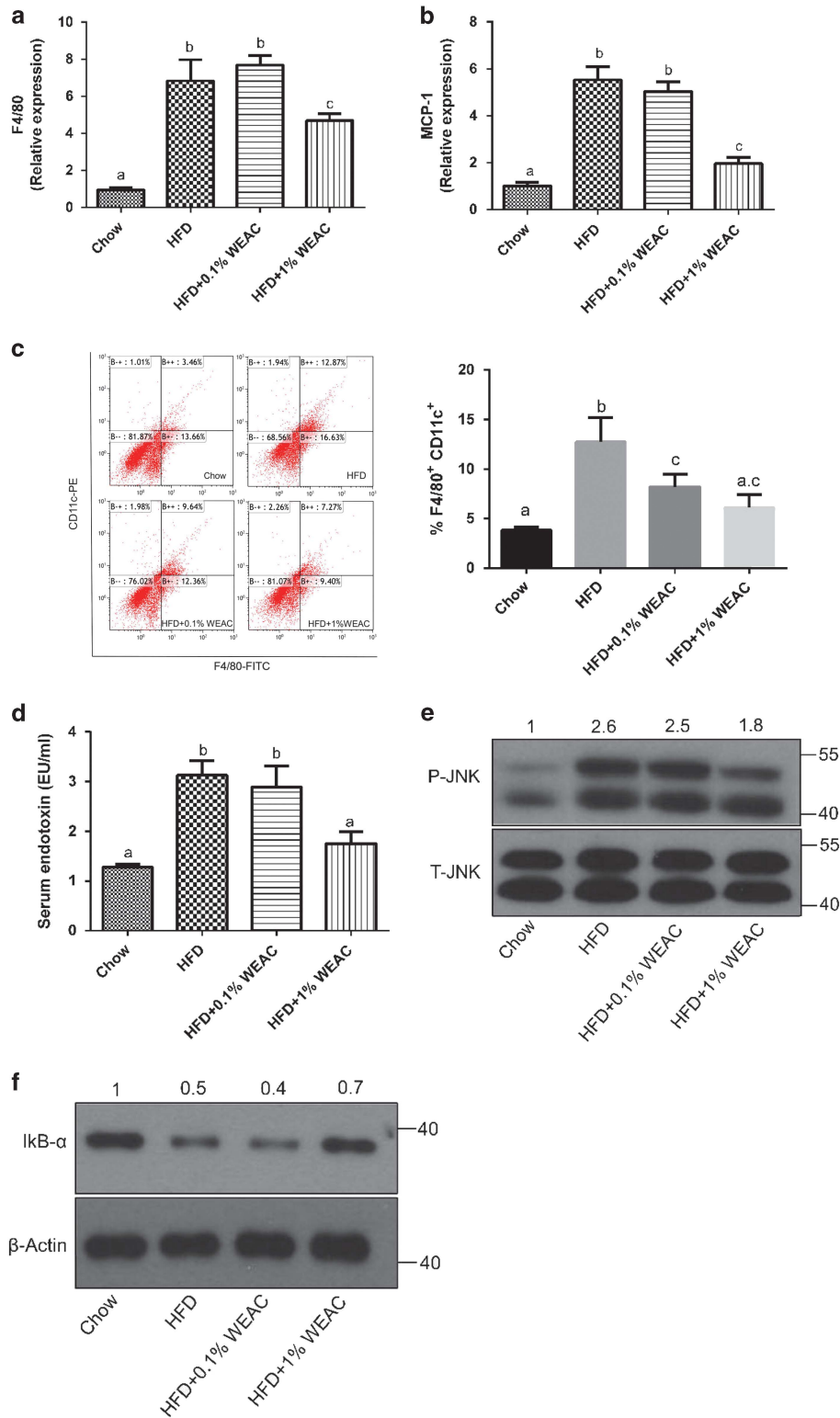


**Figure 3.** WEAC reduces macrophage infiltration, serum endotoxin and pro-inflammatory signaling pathways in HFD-fed mice. Effects of WEAC on mRNA expression levels of F4/80 (**a**) and MCP-1 (**b**) in EAT as assessed by qRT-PCR ( $n = 5$  for each group). Mice were treated as in Figure 1. Relative mRNA expression levels represent means  $\pm$  s.d. Expression level was normalized against GAPDH. Macrophage infiltration in EAT (**c**) was determined by flow cytometry; quantification is shown in the panel on the right. Effect of WEAC on serum endotoxin (LPS) (**d**) was assessed using the limulus amoebocyte lysate assay kit and expressed as means  $\pm$  s.d. of serum endotoxin units per ml. Effects of WEAC on P-JNK (**e**) and I $\kappa$ B- $\alpha$  (**f**) was assessed using Western blotting. In **e**, the anti-JNK antibodies (P-JNK and T-JNK) react against the two JNK isoforms p54 and p46. In **e** and **f**, relative band intensities for P-JNK and I $\kappa$ B- $\alpha$  were determined by densitometry analysis (values shown on top of each blot; for P-JNK, the values represent the average intensity of the two bands). Graph bars with different letters on top correspond to statistically significant results ( $P < 0.05$ ) based on Bonferroni *post hoc* one-way ANOVA analysis.

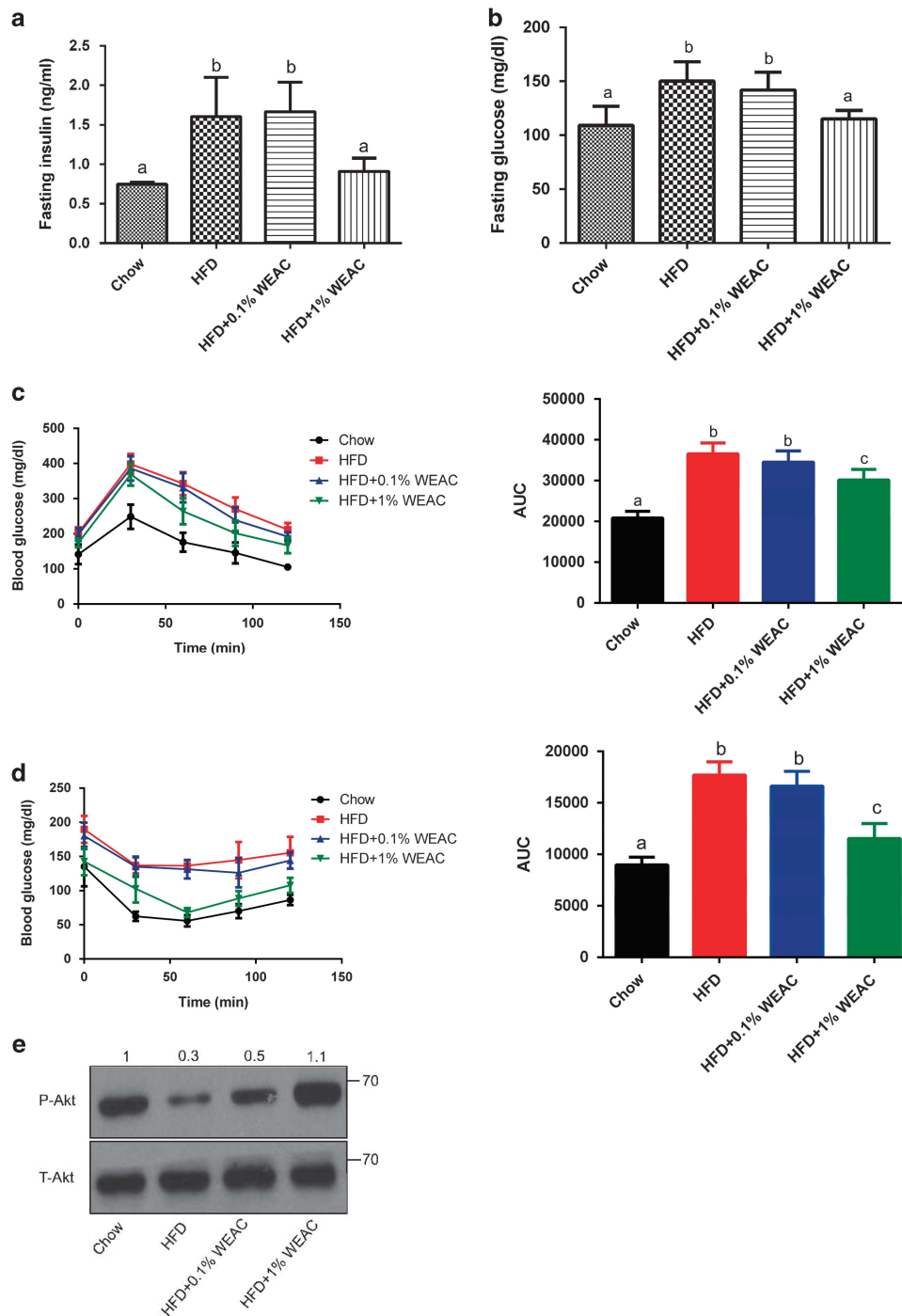


**Figure 4.** WEAC supplementation reduces HFD-induced insulin resistance. Effects of WEAC on fasting insulin (a), fasting glucose (b), oral glucose tolerance test (c), insulin tolerance test (d) and phosphorylation of Akt in EAT (e) ( $n = 5$  for each group). T-Akt refers to total Akt. Insulin and glucose levels were monitored using commercial ELISA kit and a glucose meter, respectively. The areas under the curve (AUC) in (c, d) (right panels) are also shown. Graph bars with different letters on top correspond to statistically significant results ( $P < 0.05$ ) based on Bonferroni *post hoc* one-way ANOVA analysis. In e, relative P-Akt band intensities determined by densitometry analysis are shown on top.

agreement with previous studies, taxonomic profiling showed that the ratio of Firmicutes to Bacteroidetes (F/B ratio) increased following HFD feeding (Figure 6b). In contrast, WEAC treatment (1%) reduced the F/B ratio to a level similar to that observed in chow-fed mice (Figure 6b).

Compared with HFD-fed mice, WEAC supplementation (1%) increased the level of several bacterial species, some of which have been shown to produce beneficial effects on obesity and

inflammation, including *Streptococcus* spp.,<sup>42</sup> *Eubacterium* spp.,<sup>43</sup> *Eggerthella lenta*,<sup>44</sup> *Clostridium* IV (*Clostridium methylpentosum*)<sup>25</sup> and *A. muciniphila*<sup>18</sup> (Figure 6c; see also Supplementary Table 2). In contrast, Ruminococcaceae and Lachnospiraceae at the family level and *Clostridium scindens* and *Clostridium cocleatum* at the species level were reduced by WEAC treatment (1%) compared with the HFD group (Figure 6c and Supplementary Table 2). Together, these results indicate that WEAC administration alters

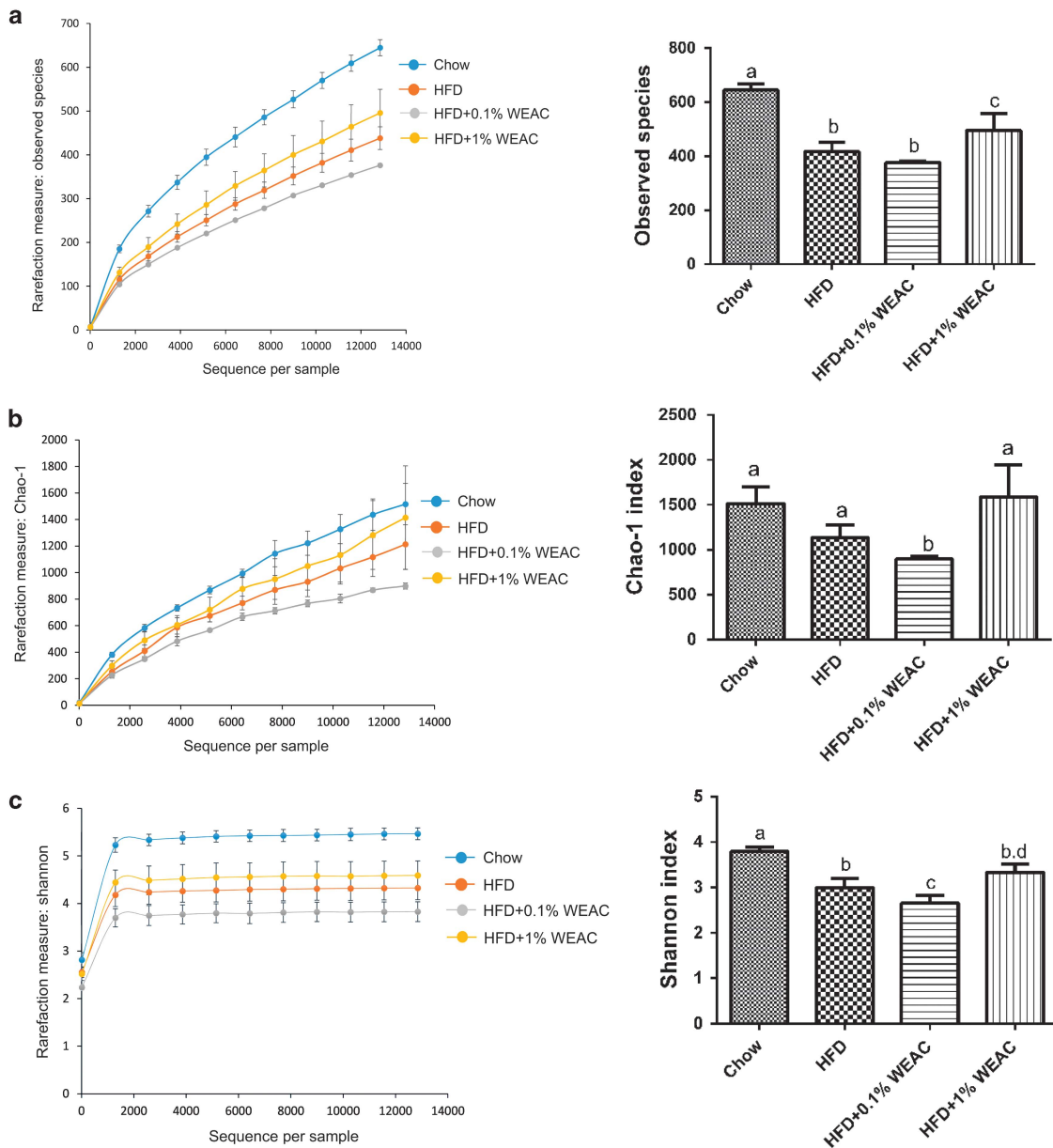


**Figure 5.** Diversity analysis of WEAC-treated gut microbiota. Observed species (a), Chao-1 index (b) and Shannon index (c) of fecal samples from mice fed with chow ( $n=4$ ), HFD ( $n=4$ ), HFD+0.1% WEAC ( $n=4$ ) or HFD+1% WEAC ( $n=3$ ). Graph bars with different letters on top correspond to statistically significant results ( $P < 0.05$ ) based on Bonferroni *post hoc* one-way ANOVA analysis.

the gut microbiota community, an observation that may explain at least in part the beneficial effects of this extract on obesity and inflammation.

## DISCUSSION

Although previous studies have shown that *A. cinnamomea* may reduce lipid accumulation in rodents,<sup>12–14</sup> the mechanism underlying this effect and whether the mushroom may modulate the composition of the gut microbiota or intestinal integrity remained unclear. In the present study, we showed that WEAC reduces body weight and obesity-associated metabolic disorders in HFD-fed mice by affecting a wide range of physiological processes, including lipid storage, adipokine production, macrophage infiltration, insulin sensitivity, maintenance of intestinal integrity and gut microbiota composition. Our findings suggest that

*A. cinnamomea* may represent a new anti-obesogenic and antidiabetic treatment.

Our previous study<sup>25</sup> showed that *G. lucidum* possesses anti-obesogenic and antidiabetic properties similar to the effects described here for *A. cinnamomea*. In the case of *G. lucidum*, a fraction containing high molecular weight polysaccharides produced anti-obesogenic and antidiabetic effects like those of the water extract studied here. Chen *et al.*<sup>45</sup> reported that *A. cinnamomea* mycelium contains 8% polysaccharides. On the other hand, our mycelium contains 1.5% polysaccharides (before water extraction), suggesting that the effects described here may be due to other compounds, a possibility which requires further investigation. Of note, toxicological studies showed that *A. cinnamomea* produces no pathological abnormalities in Sprague–Dawley rats and BALB/c mice following consumption of high doses for 90 days (3000 mg kg<sup>-1</sup> per day and 1666.67 mg kg<sup>-1</sup> per day, respectively).<sup>45,46</sup> These

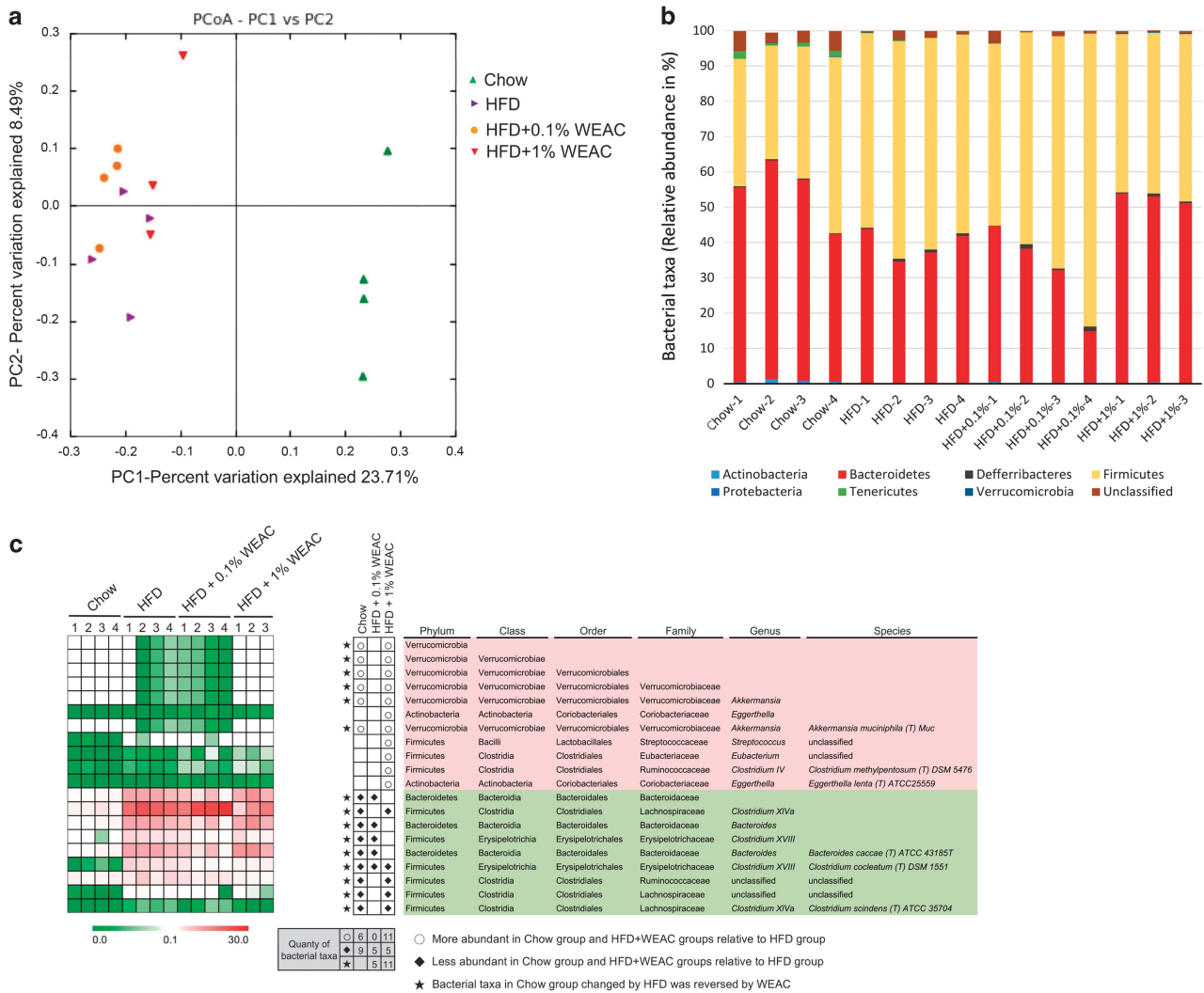


**Figure 6.** WEAC supplementation alters microbiota composition in HFD-fed mice. Microbiota composition in feces of chow-fed mice ( $n = 4$ ), HFD mice ( $n = 4$ ) treated with 0.1% ( $n = 4$ ) or 1% WEAC ( $n = 3$ ) was analyzed using next-generation sequencing and bioinformatics analysis. (a) UniFrac-based PCoA plots. (b) Bacterial taxonomic profiling of intestinal bacteria from different mouse groups at the phylum level. (c) Heat map showing the abundance of bacterial taxa significantly altered by WEAC in HFD-fed mice. Bacterial taxa information (phylum, class, order, family, genus and species) is shown in the right panel. White circles and black diamonds indicate the bacterial taxa that respectively increased and decreased in chow-fed and HFD+WEAC-fed groups compared with the HFD-fed group. Black stars represent bacterial taxa whose abundance in chow-fed mice was altered by HFD and reversed by WEAC.

observations suggest that *A. cinnamomea* may be suitable for long-term use.

We observed that WEAC supplementation reduces the expression of enzymes involved in lipid synthesis (ACC-1, FAS and SREBP-1c) in EAT of HFD-fed mice, whereas it increases the expression of proteins involved in lipid oxidation (PGC-1 $\alpha$ ). ACC-1 is a biotin-dependent enzyme that catalyzes the irreversible carboxylation of acetyl-CoA to produce malonyl-CoA, which is a substrate for FAS to generate palmitate.<sup>47</sup> Upon activation, SREBP-1c translocates from the cytosol into the nucleus, where it acts as a transcription factor and binds to specific sterol regulatory DNA sequences, thereby upregulating the synthesis of enzymes involved in sterol biosynthesis.<sup>48</sup> Reduced expression of these three proteins may be involved in the reduced fat accumulation and fatty acid levels observed in WEAC-treated mice (Figure 1 and Supplementary Figure 3). In contrast, PGC-1 $\alpha$  interacts with the nuclear receptor PPAR- $\gamma$ , resulting in recruitment of other transcription factors and co-activators.<sup>48</sup> As PGC-1 $\alpha$  is a key regulator of energy metabolism, upregulation of this transcriptional co-activator following WEAC supplementation

(Supplementary Figure 3d) is consistent with increased energy consumption.<sup>49</sup> These results suggest that WEAC may reduce fat accumulation and blood lipid levels by modulating enzymes and proteins involved in lipid metabolism.

The Akt enzyme, also known as protein kinase B, is a serine/threonine protein kinase that has a key role in several cellular processes, including glucose metabolism, cell proliferation and cell migration.<sup>50</sup> Previous studies have shown that over-production of pro-inflammatory cytokines such as TNF- $\alpha$ , IL-1 $\beta$ , IL-6 and MCP-1 in obese animals may be responsible for the development of chronic inflammation and insulin resistance, owing at least in part to deregulation of the Akt pathway in muscle cells and immune cells.<sup>35</sup> In the present study, we observed that WEAC supplementation reduces the production of pro-inflammatory cytokines (Figure 2) and enhances phosphorylation of Akt (Figure 4e), which may explain the improved insulin sensitivity observed in the treated mice.

Following stimulation of Toll-like receptors by pathogen-associated molecular patterns, such as peptidoglycan and LPS from bacteria, intestinal Paneth cells can produce Reg3g.<sup>40</sup>

Previous work showed that Reg3g-deficient mice have an altered intestinal mucus distribution and show signs of mucosal inflammation in response to the gut microbiota,<sup>51</sup> findings that highlight the important role of Reg3g in controlling gut microbiota homeostasis. Lysozyme C functions by attacking peptidoglycans found in the bacterial cell wall. The level of this protein correlates inversely with body weight and its reduction appears to represent an important alteration that affects the microbiota of obese individuals.<sup>52</sup> In contrast, the enzyme Pla2g2 releases fatty acids from phospholipids found in the cell membrane and can induce the production of pro-inflammatory eicosanoids.<sup>53</sup> Our results showed that WEAC increased the expression of Reg3g and lysozyme C in the ileum of HFD-fed mice, whereas no effect was observed for PLA2g2 (Supplementary Figure 4). These results indicate that WEAC enhances host antimicrobial defense mechanisms, which may further explain the modulatory effects of WEAC on the gut microbiota.

Macrophages can exhibit either pro- or anti-inflammatory phenotypes and are generally grouped as M1 or M2 phenotypes.<sup>33</sup> M1 macrophages secrete pro-inflammatory cytokines, such as TNF- $\alpha$ , IL-6, and IL-1 $\beta$ , and are involved in the pro-inflammatory response. In contrast, M2 macrophages mainly secrete anti-inflammatory cytokines, such as IL-10, TGF- $\beta$  and IL-4, and are involved in wound healing and termination of the inflammatory response.<sup>33</sup> Adipose tissue macrophages refer to tissue-resident macrophages found in adipose tissues. In both humans and rodents, macrophages may accumulate in adipose tissues upon increased body weight, and may act as major contributors to tissue inflammation and insulin resistance in obese individuals.<sup>33</sup> Besides, the number of macrophages within adipose tissues depends on the metabolic status of the host. Previous work has shown that the percentage of macrophages within adipose tissues ranges from 10% in lean mice and humans to 50% in extremely obese, leptin-deficient mice (almost 40% in obese humans).<sup>54</sup> The increased number of adipose tissue macrophages, namely the pro-inflammatory M1 macrophages, correlates with increased production of pro-inflammatory cytokines by adipose tissues, a phenomenon that might contribute to the pathological effects of weight gain and obesity.<sup>33</sup> Cytokines and chemokines such as MCP-1 are also involved in regulating migration and infiltration of monocytes/macrophages. In addition, pro-inflammatory cytokines such as TNF- $\alpha$  are mostly produced by macrophages rather than adipocytes.<sup>54</sup> It has been proposed that pro-inflammatory cytokines and macrophages may contribute to the development of insulin resistance and type 2 diabetes in obese animals. Importantly, WEAC supplementation reduced the levels of pro-inflammatory cytokines and adipose tissue macrophages (Figures 2 and 3), which may also contribute to the beneficial effect of the extract on obesity.

WEAC treatment enhanced adiponectin signaling, as shown by activation of AMPK (Supplementary Figure 2). AMPK is involved in many important physiological functions in animals and humans, including activation of fatty-acid oxidation in the liver and muscles, increased production of ketone bodies, reduced cholesterol production, enhanced muscle glucose uptake and modulation of insulin secretion by pancreatic beta-cells.<sup>55</sup> Many of the effects of WEAC, including reduced body weight and fat accumulation (Figure 1) and amelioration of insulin resistance (Figure 4), may be attributed at least in part to AMPK activation.

Effective preventive or therapeutic strategies that can reduce the development of chronic low-grade inflammation and insulin resistance would be beneficial to prevent type 2 diabetes and obesity. Many prebiotics are non-digestible polysaccharides that are fermented by bacteria in the colon to produce short-chain fatty acids that can be absorbed into the blood in order to regulate various physiological functions, including lipid metabolism and immunity.<sup>26</sup> We have previously reported that high molecular weight polysaccharides purified from a water extracts of

*G. lucidum* reduce body weight and obesity-related disorders in HFD-fed mice.<sup>25</sup> In the present study, we observed that WEAC produced significant changes on the gut microbiota of HFD-fed mice (Figures 5 and 6). WEAC significantly reduced the Firmicutes-to-Bacteroidetes ratio in HFD-fed mice (Figure 6b), consistent with previous observations of mushroom-derived prebiotics.<sup>25</sup> WEAC supplementation also reversed the effects of HFD on several bacterial taxa associated with weight loss (Figure 6c and Supplementary Table 2). Previous studies have shown that the gut microbiota is closely involved in the development of obesity in animals.<sup>17</sup> For example, an increased number of *C. methylpentosum* (Clostridium IV) was observed following treatment with *G. lucidum* polysaccharides.<sup>25</sup> Moreover, in rats fed with a HFD or a high-sucrose diet rat, treatment with trans-resveratrol increased *C. methylpentosum* and reduced aberrant phenotypes in the gut microbiota.<sup>56</sup> Another study showed that *A. muciniphila* can reduce obesity and restore intestinal barrier functions by regulating inflammation and lipid metabolism.<sup>18</sup> Upon treatment with the prebiotic oligofructose, *A. muciniphila* also increased intestinal Reg3g expression.<sup>18</sup> Furthermore, *Eubacterium* spp. induced by prebiotic oligosaccharides produced beneficial effects on animals.<sup>43</sup> *Eggerthella lenta* was enriched by red wine polyphenols that improve metabolic syndrome in patients.<sup>44</sup> *Streptococcus* spp. are also considered as having probiotic properties.<sup>42</sup> Our results demonstrate that WEAC supplementation enriches *C. methylpentosum*, *A. muciniphila*, *Eubacterium* spp. and *Streptococcus* spp. in HFD-fed obese mice (Figure 6c). These results suggest that the effects of WEAC may be due, at least in part, to an increase in these gut bacterial species.

On the other hand, several bacterial species have been associated with a pro-inflammatory response and weight gain. For example, *Bacteroides caccae* is an opportunistic pathogen whose level correlates with type 2 diabetes mellitus and inflammation.<sup>57</sup> *C. cocleatum* is positively correlated with LPS levels and progression of liver disease in streptozotocin-HFD-fed animals.<sup>58</sup> *Clostridium scindens* is enriched by HFD feeding and is associated with increased amounts of deoxycholic acid, which may cause inflammation and liver cancer.<sup>59</sup> In addition, *Ruminococcaceae* and *Lachnospiraceae* at the family level were both enhanced in HFD-fed mice.<sup>60</sup> Of note, WEAC supplementation reduced the levels of these bacteria (Figure 6c and Supplementary Table 2). Therefore, WEAC may prevent HFD-induced obesity and complications by modulating the composition of the gut microbiota in multiple ways.

Taken together, our results indicate that *A. cinnamomea* possesses anti-obesogenic, antidiabetic and anti-inflammatory properties in an animal model of diet-induced obesity. Further studies are needed to identify the active compounds responsible for these effects and to test the effects of *A. cinnamomea* in humans.

## CONFLICT OF INTEREST

Y-FK is President of Chang Gung Biotechnology. JDY is Chairman of the Board of Chang Gung Biotechnology. The authors have filed patent applications related to the preparation and use of medicinal mushrooms and probiotics.

## ACKNOWLEDGEMENTS

The authors' work is supported by Primordia Institute of New Sciences and Medicine, by grants MOST105-2320-B-030-004 and MOST105-2320-B-182-032-MY3 from the Ministry of Science and Technology of Taiwan, and by grants CMRPD1F0121-3 and CORPD1F0011-3 from Chang Gung Memorial Hospital.

## REFERENCES

- Allison DB, Downey M, Atkinson RL, Billington CJ, Bray GA, Eckel RH et al. Obesity as a disease: a white paper on evidence and arguments commissioned by the Council of the Obesity Society. *Obesity (Silver Spring)* 2008; **16**: 1161–1177.

- 2 Collaboration NCDRF. Trends in adult body-mass index in 200 countries from 1975 to 2014: a pooled analysis of 1698 population-based measurement studies with 19.2 million participants. *Lancet* 2016; **387**: 1377–1396.
- 3 Osborn O, Olefsky JM. The cellular and signaling networks linking the immune system and metabolism in disease. *Nat Med* 2012; **18**: 363–374.
- 4 Odegaard JI, Chawla A. Pleiotropic actions of insulin resistance and inflammation in metabolic homeostasis. *Science* 2013; **339**: 172–177.
- 5 Martel J, Ojcius DM, Lai HC, Young JD. Mushrooms - from cuisine to clinic. *Biomed J* 2014; **37**: 343–344.
- 6 Wasser SP. Medicinal mushroom science: current perspectives, advances, evidences, and challenges. *Biomed J* 2014; **37**: 345–356.
- 7 Chang TT, Chou WN. *Antrodia cinnamomea* sp. nov. on *Cinnamomum kanehirai* in Taiwan. *Mycol Res* 1995; **99**: 756–758.
- 8 Huang TH, Chiu YH, Chan YL, Wang H, Li TL, Liu CY et al. *Antrodia cinnamomea* alleviates cisplatin-induced hepatotoxicity and enhances chemo-sensitivity of line-1 lung carcinoma xenografted in BALB/cByJ mice. *Oncotarget* 2015; **6**: 25741–25754.
- 9 Geethangili M, Tzeng YM. Review of pharmacological effects of *Antrodia camphorata* and its bioactive compounds. *Evid Based Complement Alternat Med* 2011; **2011**: 121641.
- 10 Song TY, Yen GC. Protective effects of fermented filtrate from *Antrodia camphorata* in submerged culture against CCl4-induced hepatic toxicity in rats. *J Agric Food Chem* 2003; **51**: 1571–1577.
- 11 Huang TT, Wu SP, Chong KY, Ojcius DM, Ko YF, Wu YH et al. The medicinal fungus *Antrodia cinnamomea* suppresses inflammation by inhibiting the NLRP3 inflammasome. *J Ethnopharmacol* 2014; **155**: 154–164.
- 12 Lai MN, Ko HJ, Ng LT. Hypolipidemic effects of *Antrodia cinnamomea* extracts in high-fat diet-fed hamsters. *J Food Biochem* 2012; **36**: 233–239.
- 13 Kuo YH, Lin CH, Shih CC. Ergostatrien-3beta-ol from *Antrodia camphorata* inhibits diabetes and hyperlipidemia in high-fat-diet treated mice via regulation of hepatic related genes, glucose transporter 4, and AMP-activated protein kinase phosphorylation. *J Agric Food Chem* 2015; **63**: 2479–2489.
- 14 Kuo YH, Lin CH, Shih CC. Antidiabetic and antihyperlipidemic properties of a triterpenoid compound, dehydroeburicoic acid, from *Antrodia camphorata* in vitro and in streptozotocin-induced mice. *J Agric Food Chem* 2015; **63**: 10140–10151.
- 15 Zhao L. The gut microbiota and obesity: from correlation to causality. *Nat Rev Microbiol* 2013; **11**: 639–647.
- 16 Lin CS, Chang CJ, Lu CC, Martel J, Ojcius DM, Ko YF et al. Impact of the gut microbiota, prebiotics, and probiotics on human health and disease. *Biomed J* 2014; **37**: 259–268.
- 17 Ridaura VK, Faith JJ, Rey FE, Cheng J, Duncan AE, Kau AL et al. Gut microbiota from twins discordant for obesity modulate metabolism in mice. *Science* 2013; **341**: 1241214.
- 18 Everard A, Belzer C, Geurts L, Ouwerkerk JP, Druart C, Bindels LB et al. Cross-talk between *Akkermansia muciniphila* and intestinal epithelium controls diet-induced obesity. *Proc Natl Acad Sci USA* 2013; **110**: 9066–9071.
- 19 Cani PD, Bibiloni R, Knauf C, Waget A, Neyrinck AM, Delzenne NM et al. Changes in gut microbiota control metabolic endotoxemia-induced inflammation in high-fat diet-induced obesity and diabetes in mice. *Diabetes* 2008; **57**: 1470–1481.
- 20 Cani PD, Amar J, Iglesias MA, Poggi M, Knauf C, Bastelica D et al. Metabolic endotoxemia initiates obesity and insulin resistance. *Diabetes* 2007; **56**: 1761–1772.
- 21 Delzenne NM, Neyrinck AM, Backhed F, Cani PD. Targeting gut microbiota in obesity: effects of prebiotics and probiotics. *Nat Rev Endocrinol* 2011; **7**: 639–646.
- 22 Wang J, Tang H, Zhang C, Zhao Y, Derrien M, Rocher E et al. Modulation of gut microbiota during probiotic-mediated attenuation of metabolic syndrome in high fat diet-fed mice. *ISME J* 2015; **9**: 1–15.
- 23 Parnell JA, Reimer RA. Prebiotic fiber modulation of the gut microbiota improves risk factors for obesity and the metabolic syndrome. *Gut Microbes* 2012; **3**: 29–34.
- 24 Everard A, Lazarevic V, Gaia N, Johansson M, Stahlman M, Backhed F et al. Microbiome of prebiotic-treated mice reveals novel targets involved in host response during obesity. *ISME J* 2014; **8**: 2116–2130.
- 25 Chang CJ, Lin CS, Lu CC, Martel J, Ko YF, Ojcius DM et al. *Ganoderma lucidum* reduces obesity in mice by modulating the composition of the gut microbiota. *Nat Commun* 2015; **6**: 7489.
- 26 Martel J, Ojcius DM, Chang CJ, Lin CS, Lu CC, Ko YF et al. Anti-obesogenic and antidiabetic effects of plants and mushrooms. *Nature Rev Endocrinol* 2017; **13**: 149–160.
- 27 Rossi J, Herzig KH, Voikar V, Hiltunen PH, Segerstrale M, Airaksinen MS. Alimentary tract innervation deficits and dysfunction in mice lacking GDNF family receptor alpha2. *J Clin Invest* 2003; **112**: 707–716.
- 28 Kozich JJ, Westcott SL, Baxter NT, Highlander SK, Schloss PD. Development of a dual-index sequencing strategy and curation pipeline for analyzing amplicon sequence data on the MiSeq Illumina sequencing platform. *Appl Environ Microbiol* 2013; **79**: 5112–5120.
- 29 DeSantis Jr TZ, Hugenholtz P, Keller K, Brodie EL, Larsen N, Piceno YM et al. NAST: a multiple sequence alignment server for comparative analysis of 16S rRNA genes. *Nucleic Acids Res* 2006; **34**: W394–W399.
- 30 Edgar RC, Haas BJ, Clemente JC, Quince C, Knight R. UCHIME improves sensitivity and speed of chimera detection. *Bioinformatics* 2011; **27**: 2194–2200.
- 31 Caporaso JG, Kuczynski J, Stombaugh J, Bittinger K, Bushman FD, Costello EK et al. QIIME allows analysis of high-throughput community sequencing data. *Nat Methods* 2010; **7**: 335–336.
- 32 Benjamini Y, Krieger AM, Yekutieli D. Adaptive linear step-up procedures that control the false discovery rate. *Biometrika* 2006; **93**: 491–507.
- 33 Fujisaka S, Usui I, Bukhari A, Iktani M, Oya T, Kanatani Y et al. Regulatory mechanisms for adipose tissue M1 and M2 macrophages in diet-induced obese mice. *Diabetes* 2009; **58**: 2574–2582.
- 34 Chawla A, Nguyen KD, Goh YP. Macrophage-mediated inflammation in metabolic disease. *Nat Rev Immunol* 2011; **11**: 738–749.
- 35 Kahn SE, Hull RL, Utzschneider KM. Mechanisms linking obesity to insulin resistance and type 2 diabetes. *Nature* 2006; **444**: 840–846.
- 36 Tilg H, Moschen AR. Adipocytokines: mediators linking adipose tissue, inflammation and immunity. *Nat Rev Immunol* 2006; **6**: 772–783.
- 37 Strable MS, Ntambi JM. Genetic control of de novo lipogenesis: role in diet-induced obesity. *Crit Rev Biochem Mol Biol* 2010; **45**: 199–214.
- 38 Srivastava RA, Pinkosky SL, Filippov S, Hanselman JC, Cramer CT, Newton RS. AMP-activated protein kinase: an emerging drug target to regulate imbalances in lipid and carbohydrate metabolism to treat cardio-metabolic diseases. *J Lipid Res* 2012; **53**: 2490–2514.
- 39 Shi H, Kokoeva MV, Inouye K, Tzameli I, Yin H, Flier JS. TLR4 links innate immunity and fatty acid-induced insulin resistance. *J Clin Invest* 2006; **116**: 3015–3025.
- 40 Ostaff MJ, Stange EF, Wehkamp J. Antimicrobial peptides and gut microbiota in homeostasis and pathology. *EMBO Mol Med* 2013; **5**: 1465–1483.
- 41 Le Chatelier E, Nielsen T, Qin J, Prifti E, Hildebrand F, Falony G et al. Richness of human gut microbiome correlates with metabolic markers. *Nature* 2013; **500**: 541–546.
- 42 Fijan S. Microorganisms with claimed probiotic properties: an overview of recent literature. *Int J Environ Res Public Health* 2014; **11**: 4745–4767.
- 43 Roberfroid M, Gibson GR, Hoyles L, McCartney AL, Rastall R, Rowland I et al. Prebiotic effects: metabolic and health benefits. *Br J Nutr* 2010; **104**: S1–63.
- 44 Moreno-Indias I, Sanchez-Alcoholado L, Perez-Martinez P, Andres-Lacueva C, Cardona F, Tinahones F et al. Red wine polyphenols modulate fecal microbiota and reduce markers of the metabolic syndrome in obese patients. *Food Funct* 2016; **7**: 1775–1787.
- 45 Chen TI, Chen CC, Lin TW, Tsai YT, Nam MK. A 90-day subchronic toxicological assessment of *Antrodia cinnamomea* in Sprague-Dawley rats. *Food Chem Toxicol* 2011; **49**: 429–433.
- 46 Chang JB, Wu MF, Lu HF, Chou J, Au MK, Liao NC et al. Toxicological evaluation of *Antrodia cinnamomea* in BALB/c mice. *In Vivo* 2013; **27**: 739–745.
- 47 Wakil SJ, Abu-Elheiga LA. Fatty acid metabolism: target for metabolic syndrome. *J Lipid Res* 2009; **50**: S138–43.
- 48 Wang X, Sato R, Brown MS, Hua X, Goldstein JL. SREBP-1, a membrane-bound transcription factor released by sterol-regulated proteolysis. *Cell* 1994; **77**: 53–62.
- 49 Jun HJ, Joshi Y, Patil Y, Noland RC, Chang JS. NT-PGC-1alpha activation attenuates high-fat diet-induced obesity by enhancing brown fat thermogenesis and adipose tissue oxidative metabolism. *Diabetes* 2014; **63**: 3615–3625.
- 50 Liao Y, Hung MC. Physiological regulation of Akt activity and stability. *Am J Transl Res* 2010; **2**: 19–42.
- 51 Loonen LM, Stolte EH, Jaklofsky MT, Meijerink M, Dekker J, van Baarlen P et al. REG3gamma-deficient mice have altered mucus distribution and increased mucosal inflammatory responses to the microbiota and enteric pathogens in the ileum. *Mucosal Immunol* 2014; **7**: 939–947.
- 52 Hodin CM, Verdam FJ, Grootjans J, Rensen SS, Verheyen FK, Dejong CH et al. Reduced Paneth cell antimicrobial protein levels correlate with activation of the unfolded protein response in the gut of obese individuals. *J Pathol* 2011; **225**: 276–284.
- 53 Tithof PK, Peters-Golden M, Ganey PE. Distinct phospholipases A2 regulate the release of arachidonic acid for eicosanoid production and superoxide anion generation in neutrophils. *J Immunol* 1998; **160**: 953–960.
- 54 Weisberg SP, McCann D, Desai M, Rosenbaum M, Leibel RL, Ferrante AW Jr. Obesity is associated with macrophage accumulation in adipose tissue. *J Clin Invest* 2003; **112**: 1796–1808.
- 55 Daval M, Fougelle F, Ferre P. Functions of AMP-activated protein kinase in adipose tissue. *J Physiol* 2006; **574**: 55–62.
- 56 Etxeberria U, Arias N, Boque N, Macarulla MT, Portillo MP, Martinez JA et al. Reshaping faecal gut microbiota composition by the intake of trans-resveratrol and quercetin in high-fat sucrose diet-fed rats. *J Nutr Biochem* 2015; **26**: 651–660.

- 57 Hakansson A, Molin G. Gut microbiota and inflammation. *Nutrients* 2011; **3**: 637–682.
- 58 Xie G, Wang X, Liu P, Wei R, Chen W, Rajani C *et al*. Distinctly altered gut microbiota in the progression of liver disease. *Oncotarget* 2016; **7**: 19355–19366.
- 59 Yoshimoto S, Loo TM, Atarashi K, Kanda H, Sato S, Oyadomari S *et al*. Obesity-induced gut microbial metabolite promotes liver cancer through senescence secretome. *Nature* 2013; **499**: 97–101.
- 60 Lecomte V, Kaakoush NO, Maloney CA, Raipuria M, Huinao KD, Mitchell HM *et al*. Changes in gut microbiota in rats fed a high fat diet correlate with obesity-associated metabolic parameters. *PLoS ONE* 2015; **10**: e0126931.

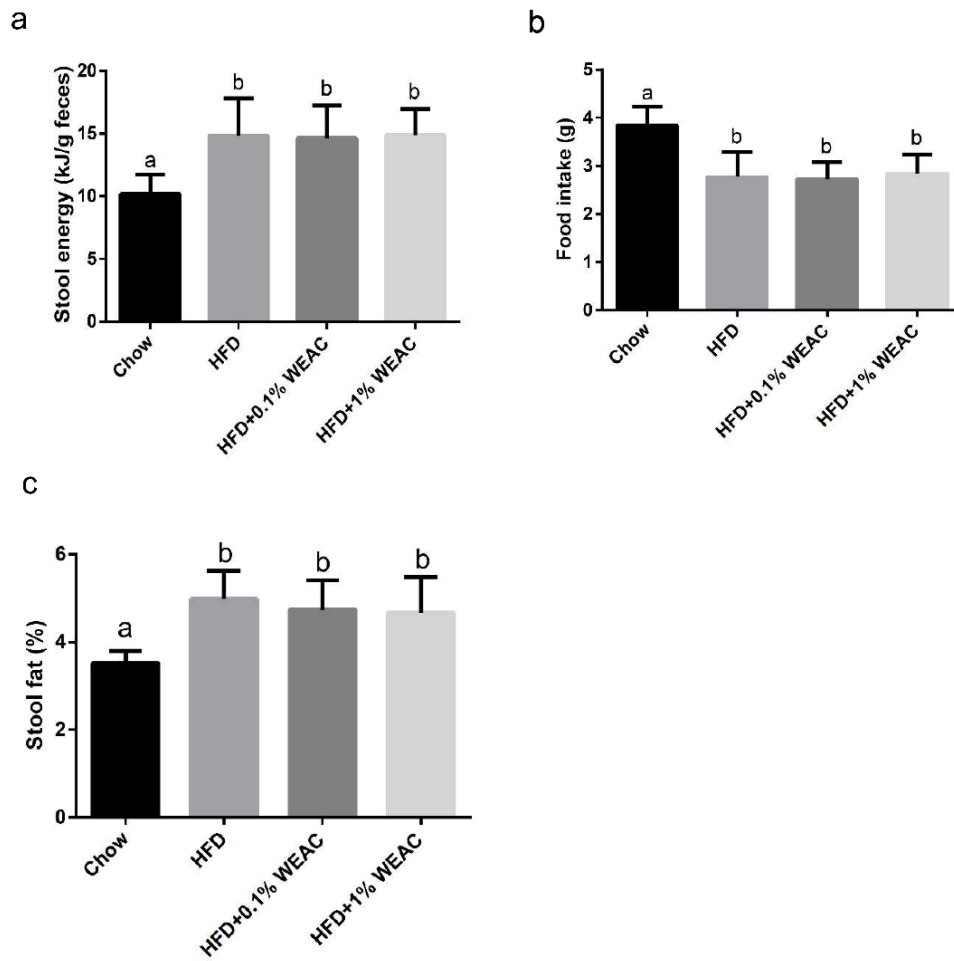


This work is licensed under a Creative Commons Attribution-NonCommercial-NoDerivs 4.0 International License. The images or other third party material in this article are included in the article's Creative Commons license, unless indicated otherwise in the credit line; if the material is not included under the Creative Commons license, users will need to obtain permission from the license holder to reproduce the material. To view a copy of this license, visit <http://creativecommons.org/licenses/by-nc-nd/4.0/>

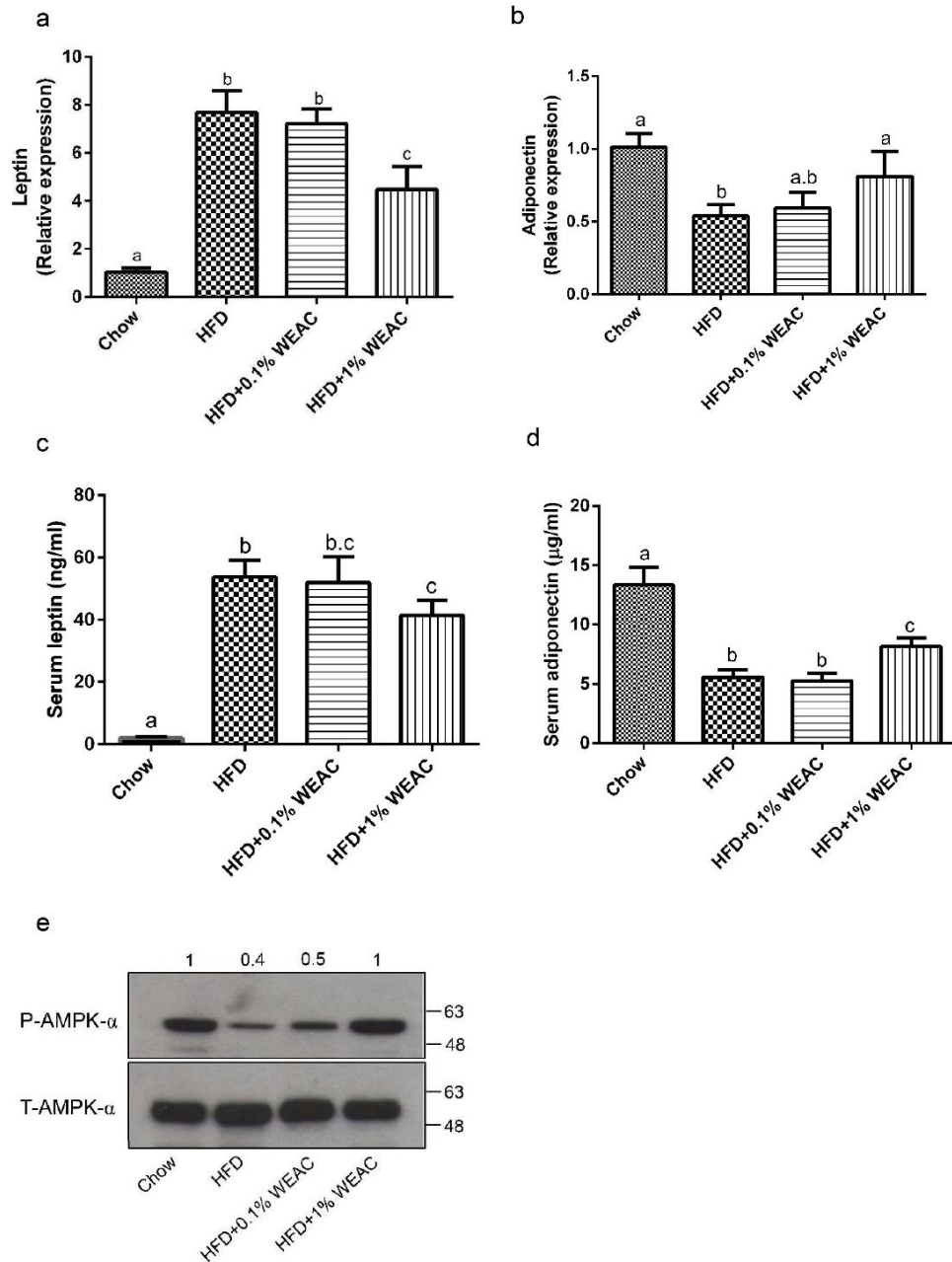
© The Author(s) 2018

Supplementary Information accompanies this paper on International Journal of Obesity website (<http://www.nature.com/ijo>)

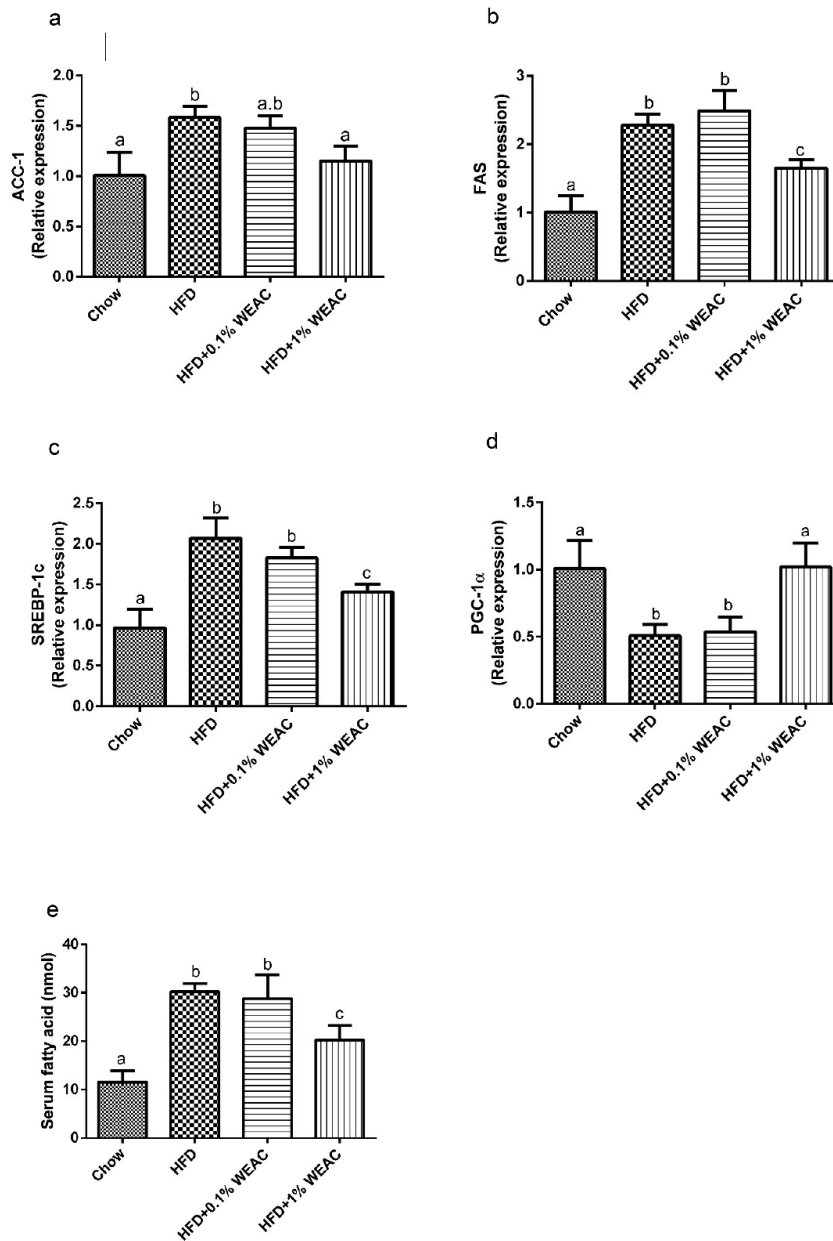
## Supplementary Figures



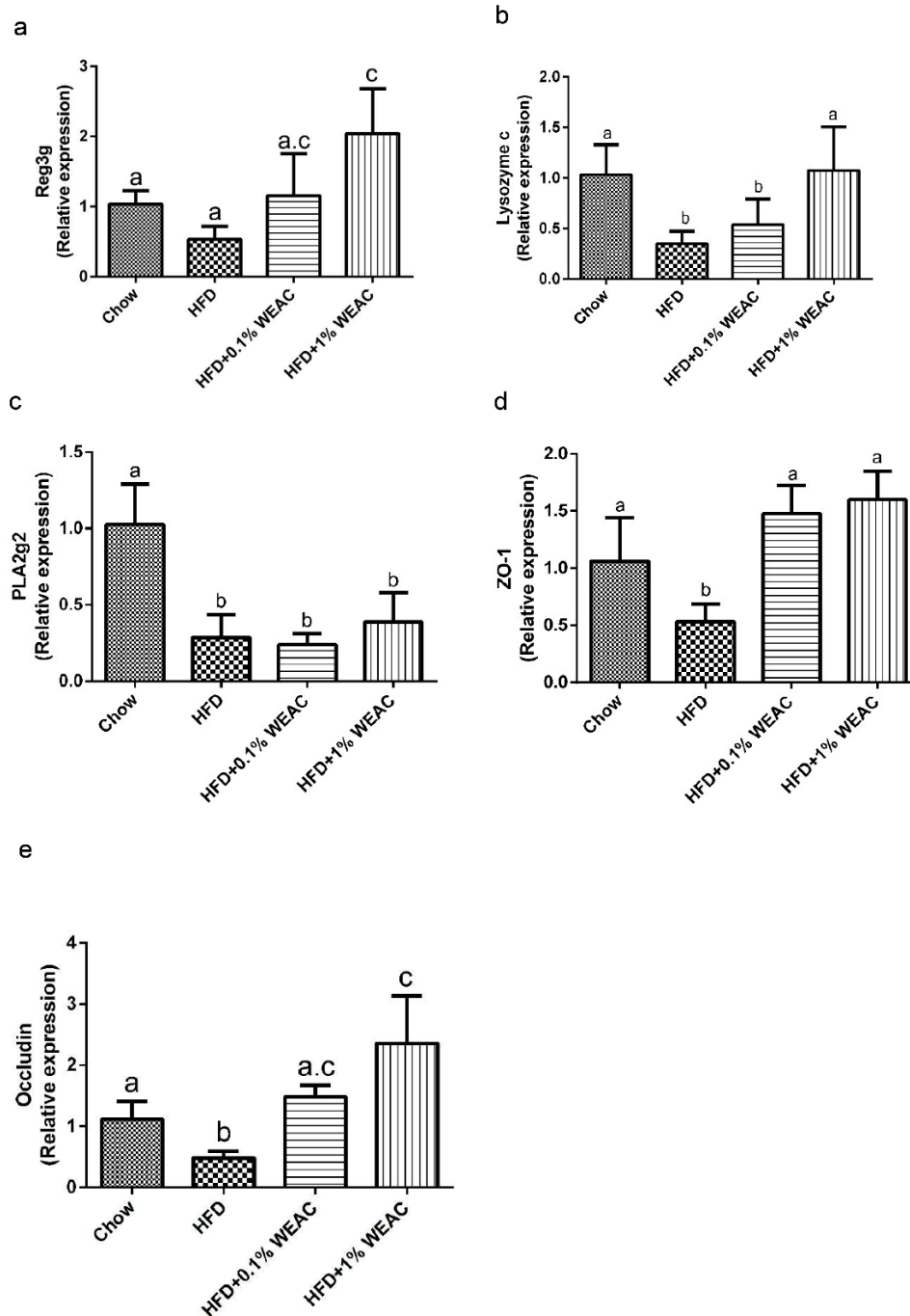
**Supplementary Figure 1.** WEAC supplementation does not influence mean energy intake, lipid absorption and energy extraction from food. Stool energy (a), food intake (b) and stool fat (c) were monitored as described in the Materials and Methods (n=5 for each group). Results are expressed as means  $\pm$  SD. Bars with different letters on top represent statistically significant results ( $P < 0.05$ ) based on Bonferroni post hoc one-way ANOVA analysis.



**Supplementary Figure 2.** WEAC treatment modulates leptin, adiponectin and phosphorylated AMPK- $\alpha$  in HFD-fed mice. Effect of WEAC treatment on leptin (a) and adiponectin (b) mRNA expression in epididymal adipose tissues (EAT) was monitored using qRT-PCR (n=5 for each group). Expression level was normalized against glyceraldehyde 3-phosphate dehydrogenase (GAPDH). Leptin (c) and adiponectin (d) protein levels were monitored using ELISA. (e) Levels of phosphorylated AMPK- $\alpha$  (P-AMPK- $\alpha$ ) and total AMPK- $\alpha$  (T-AMPK- $\alpha$ ) were determined in EAT using Western blotting. Graph bars with different letters on top represent statistically significant results ( $P < 0.05$ ) based on Bonferroni post hoc one-way ANOVA analysis.



**Supplementary Figure 3.** WEAC treatment regulates lipid metabolism in HFD-fed mice. Effects of WEAC treatment on mRNA expression of (a) acetyl-CoA carboxylase-1 (ACC-1), (b) fatty acid synthase (FAS), (c) sterol regulatory element-binding protein-1c (SREBP-1c), and (d) PPAR- $\gamma$  coactivator 1 $\alpha$  (PGC-1 $\alpha$ ) was monitored in EAT using qRT-PCR (n=5 for each group). Expression was normalized against GAPDH. Serum fatty acid level (e) was evaluated using a commercial detection kit. Graph bars with different letters on top correspond to statistically significant results ( $P < 0.05$ ) based on Bonferroni post hoc one-way ANOVA analysis.



**Supplementary Figure 4.** WEAC treatment affects the expression of antimicrobial proteins and intestinal tight junctions in HFD-fed mice. Effects of WEAC on mRNA expression levels of (a) Reg3g, (b) lysozyme C, (c) phospholipase A2 group II (PLA2g2), (d) ZO-1, and (e) occludin. Expression was normalized against GAPDH. Relative mRNA expression represents mean  $\pm$  SD as assessed by qRT-PCR (Chow, n=4; HFD, n=5; HFD+0.1% WEAC, n=4; HFD+1% WEAC, n=4). Graph bars with different letters on top represent statistically significant results ( $P < 0.05$ ) based on Bonferroni post hoc one-way ANOVA analysis.

International  
Journal of **Obesity**

nature publishing group 